

Article

Tower Configuration Impacts on the Thermal and Flow Performance of Steel-Truss Natural Draft Dry Cooling System

Huiqian Guo ¹, Yue Yang ¹, Tongrui Cheng ², Hanyu Zhou ¹, Weijia Wang ^{1,*} and Xiaoze Du ¹ 

¹ Key Laboratory of Power Station Energy Transfer Conversion and System of Ministry of Education, School of Energy Power and Mechanical Engineering, North China Electric Power University, Beijing 102206, China; 18612260421@163.com (H.G.); yangyue@ncepu.edu.cn (Y.Y.); 120171030516@ncepu.edu.cn (H.Z.); duxz@ncepu.edu.cn (X.D.)

² North China Electric Power Research Institute Co. Ltd., Beijing 100045, China; chengtr@yeah.net

* Correspondence: wangwj@ncepu.edu.cn; Tel.: +86-10-6177-3373

Abstract: In recent years, the steel-truss natural draft dry cooling technique has received attention owing to its advantages in better aseismic capability, shorter construction period, and preferable recycling. For cooling towers generating the draft force of air flow, its configuration may impact the thermal and flow performance of the steel-truss natural draft dry cooling system. With regard to the issue, this work explored the thermal and flow characteristics for the steel-truss natural draft dry cooling systems with four typical engineering tower configurations. By numerical simulation, the pressure, flow, and temperature contours were analyzed, then air mass flow rates and heat rejections were calculated and compared for the local air-cooled sectors and overall steel-truss natural draft dry cooling systems with those four tower configurations. The results present that tower 2 with the conical/cylindrical configuration had slightly lower heat rejection compared with tower 1 with the traditional hyperbolic configuration. Tower 3 with the hyperbolic/cylindrical configuration showed better thermo-flow performances than tower 1 at high crosswinds, while tower 4 with the completely cylindrical configuration appeared to have much reduced cooling capability under various crosswind conditions, along with strongly deteriorated thermal and flow behaviors. As for engineering application of the steel-truss natural draft dry cooling system, the traditional hyperbolic tower configuration is recommended for local regions with gentle wind, while for those areas with gale wind yearly, the hyperbolic/cylindrical integrated cooling tower is preferred.

Keywords: steel-truss natural draft dry cooling system; tower configuration; variable contour; thermal and flow performance; ambient crosswind



Citation: Guo, H.; Yang, Y.; Cheng, T.; Zhou, H.; Wang, W.; Du, X. Tower Configuration Impacts on the Thermal and Flow Performance of Steel-Truss Natural Draft Dry Cooling System. *Energies* **2021**, *14*, 2002. <https://doi.org/10.3390/en14072002>

Academic Editor: Luisa F. Cabeza

Received: 14 March 2021

Accepted: 25 March 2021

Published: 5 April 2021

Publisher's Note: MDPI stays neutral with regard to jurisdictional claims in published maps and institutional affiliations.



Copyright: © 2021 by the authors. Licensee MDPI, Basel, Switzerland. This article is an open access article distributed under the terms and conditions of the Creative Commons Attribution (CC BY) license (<https://creativecommons.org/licenses/by/4.0/>).

1. Introduction

In some thermal, nuclear, and solar power stations, dry-cooling systems with natural ventilation (NDDCS) have obtained extensive application because of their prominent water-saving superiority [1,2]. As the cooling system technology develops, NDDCS with the steel-truss cooling tower has been the concern of the industrial and academic fields. Compared with cooling systems with concrete towers, the steel-truss NDDCS shows better aseismic capability, shorter construction period, and preferable recycling [3]; however, its cooling performance with various typical tower configurations in engineering has not yet been revealed. Given this situation, this research will disclose the thermo-flow characteristics of the steel-truss NDDCSs with four common practical tower configurations (more details in Section 2.1), which may provide some theoretical suggestions for the thermal design of steel-truss natural draft dry cooling systems.

In recent years, research has mainly focused on exploring stability performances, connection systems, wind induced dynamic impacts, and static behaviors of the steel-truss NDDCS. Ma et al. [4] studied seven latticed tower shell systems with various grid forms, finding that the optimized construction differs for steel-truss cooling systems with

different tower heights. Geometric parameters, such as the connector type, bolt row number, and thickness of plate, were investigated, and then the proposed beam-column connections were proved with improved bending rigidity as well as ultimate bending performance [5]. On the basis of the extremely large hyperbolic steel-truss cooling system with the height of 216.3 m, which incorporates the double layers for the tower configuration, the dynamic performances were deeply revealing, pointing out that cooling towers with this steel-structure have higher natural vibration frequencies, smaller variance ratio, weaker sensitivity of dynamic response, and simpler resonant modes [6]. The stiffening rings near the tower throat and tower outlet of single-layer hyperbolic steel-truss natural draft dry cooling systems are shown to be quite necessary for enhancing the structural rigidity and stability [7].

The studies mentioned above paid close attention to handling structural design issues; however, investigations on the thermal design of steel-truss NDDCS remain scarce. Recently, a steel tower with the cylinder/frustum configuration was proposed and taken as the study object of the experiment and numerical simulation. For this steel-tower configuration, a geometric parameter of the proportion of the frustum section height to the entire tower height was recommended with a range from 0.3 to 0.5 [8]. This research can actually provide some guidelines for the cooling performance design of the steel-truss NDDCS; however, it is worth pointing out that a systematic study on clarifying thermal and flow behaviors of steel-truss natural draft dry cooling systems with various engineering tower configurations is quite necessary to promote thermal design to a further extent.

As also illustrated, most investigations of the thermo-flow performances concentrate on the concrete NDDCS with the hyperbolic tower configuration. Zhao et al. [9,10] presented specific thermal coupling of the flow contours for local cooling deltas at ambient conditions of 0 m/s, 4 m/s, and 12 m/s. Under wind speeds smaller than the critical value, Ma et al. [11] put forward a useful theoretical method to describe the heat transfer performances of NDDCS. The ambient air reverse flow near the outlet of tower will decrease the cooling capability of the cooling system [12]. Corresponding measures to improve the thermo-flow performance include water flow redistribution of the air-cooled sectors [13–15], installing windbreaker walls [16–23], and also air precooling [24–26]. Heat transfer processes for the transient start-up of cooling systems have been clearly disclosed [27–29]. Additionally, under cold ambient temperatures, the anti-freezing coupling of the thermal process of hot water and frigid air was fully studied [30–35]. The impact of the outdoor air fraction by economizer control type in cooling system loads based on real air handling unit operation parameters was disclosed, which provided references for economizer controls at hot-humid conditions [36]. Temperature fields and thermal stresses of aircraft key components of a simple geometric shape have also been studied by numerical modelling [37]. Furthermore, a mathematical model was proposed to solve convective heat transfer on the surface of typical structural elements of modern perspective aircrafts [38]. Thermo-flow investigations of these industrial units could provide some modelling references.

In conclusion, this research will carry out a thorough investigation on the thermal and flow performance of steel-truss NDDCSs with four typical engineering tower configurations, which are the traditional hyperbolic, conical/cylindrical, hyperbolic/cylindrical, and cylindrical cooling towers. With the numerical modelling method, air variable fields of various tower configurations were first analyzed, and then the mass flow rates, as well as heat rejections for local air-cooled heat exchangers (ACHE), were presented. Finally, the overall thermal and flow dimensionless parameters for all typical steel-truss cooling towers were compared. By analyzing the results, this work may offer some theoretical support for thermal design of the steel-truss NDDCS by filling the corresponding gap.

2. Numerical Modeling

2.1. Physical Model

The steel-truss NDDCSs with the four typical engineering tower configurations are shown in Figure 1. For brevity, the traditional hyperbolic tower, the conical/cylindrical tower, the hyperbolic/cylindrical tower, and the cylindrical tower are named as tower 1, tower 2, tower 3, and tower 4, respectively. These four steel-truss NDDCSs had the same dimension of ACHEs and also the same height (96.6 m) and outlet diameter (61 m) as cooling tower. The ACHE was comprised of 117 cooling deltas, which were distributed as 10 air-cooled sectors, as displayed in Figure 2. Other principal dimensions, including the height and diameter of tower throat, height of ACHE, and diameter of tower base and peripheral ACHE were 74 m and 56.4 m, 12 m, 92 m and 102.8 m, respectively.

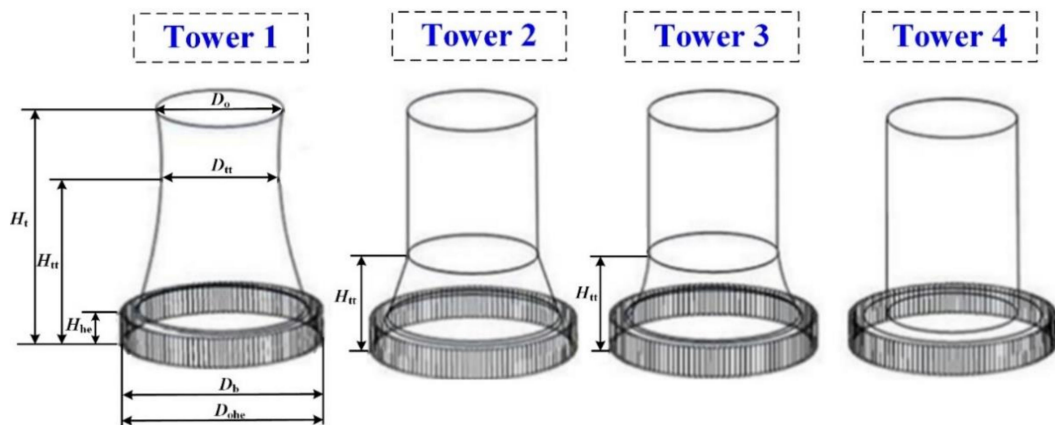


Figure 1. Steel-truss natural draft dry cooling system (NDDCSs) with different tower configurations.

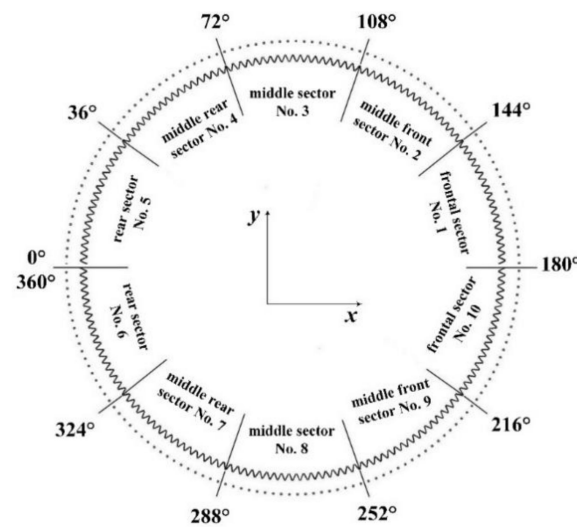


Figure 2. Schematic of air-cooled sector distribution.

2.2. Transportation Equations

The transportation equations describing the thermal and flow process of the NDDCS are summarized in the following Equation (1). In addition, the realizable $k-\epsilon$ turbulent model is employed to depict the complex air flows, because it has better performance for solving the flow recirculation, separation, and also the rotation [2,9,10].

$$\frac{\partial \rho u_j \varphi}{\partial x_j} = \frac{\partial}{\partial x_j} \left(\Gamma_\varphi \frac{\partial \varphi}{\partial x_j} \right) + S_\varphi + S_{\varphi'} \quad (1)$$

in which u_j means the air flow velocity. Symbols of φ , Γ_φ , and S_φ signify the variable term, the diffusivity term, and the source term, respectively. For ACHE zones, the additional source term S_φ' needs to be supplemented in the momentum and energy equations, which are given as follows [31]:

$$S_\varphi' = -\frac{\Delta p}{L_{x_j}} \quad (2)$$

$$S_\varphi' = \frac{\Phi_{\text{he}}}{V_{\text{he}}} \quad (3)$$

where L_{x_j} means the length in x_j direction of the cell zone of ACHE, and Φ_{he} and V_{he} mean the heat rejection and the volume of the cell zone of ACHE, respectively.

The air density inside a cooling tower varies with the air temperature according to the following equation:

$$\rho = p_{\text{ref}} \left(\frac{R}{M_a} T \right) \quad (4)$$

where ρ means the air density, T means the local air temperature, p_{ref} , R , and M_a are the reference operating pressure, universal gas constant, and the air molecular weight, respectively.

The radiator is used to express the thermal and flow characteristics of ACHE [17], in which the pressure drop as Δp is basically given as:

$$\Delta p = k_L \frac{1}{2} \rho u_f^2 \quad (5)$$

in which u_f means the air face velocity and k_L represents the air flow loss parameter, which has the function of polynomial:

$$k_L = k_L \sum_{n=1}^N r_n u_f^{n-1} \quad (6)$$

where N is given as 3, r_n means the multi-term factor with the values of 48.675, -6.305 , and 0.299, acquired from the air flow experimental test of the ACHE bundles.

For the thermal process of the radiator, the heat rejection Φ gives:

$$\Phi = h(\bar{t}_{\text{wa}} - t_{\text{a2}}) \quad (7)$$

where t_{a2} means the air outlet temperature of the ACHE and \bar{t}_{wa} equals the mean water temperature, which can be calculated by the water inlet temperature t_{wa1} and water outlet temperature t_{wa2} of the ACHE.

$$\bar{t}_{\text{wa}} = \frac{t_{\text{wa1}} + t_{\text{wa2}}}{2} \quad (8)$$

In Equation (8), both the tube conduction resistance and water convection resistance are negligible when compared with the dominant cooling air convection resistance, therefore, \bar{t}_{wa} can be regarded as the tube wall temperature. As for the convective coefficient of heat transfer h , it takes the multi-term function of:

$$h = \sum_{n=1}^N h_n u_f^{n-1} \quad (9)$$

where N equals 3, h_n means the polynomial factor with the values of 17683.43, -9167.38 , and 1938.02, acquired from the wind-tunnel test of the ACHE bundles.

2.3. Computational Domain, Boundaries and Numerical Procedure

The numerical method of computational fluid dynamics is adopted by software of ANSYS Fluent. For each steel-truss NDDCS, the domain for the numerical computation was developed with the dimension of 800 m in direction of length, 800 m in direction width, and 600 m in direction height, which presented sufficient scale to avert from the boundary impacts of ambient air [2]. As specific illustrations, Figure 3 gives the typical computational domain of tower 2 with the conical/cylindrical configuration. The multi-block meshing technique was used to generate numerical modeling grids, with structured hexahedral grids created for the ACHE and cooling tower, meanwhile the tetrahedral unstructured grids were adopted for their interval section. Furthermore, the grid interval sizes were chosen as small as 0.2 m and 2 m for key sections of the ACHE and tower shell, so as to reach the grid quality.

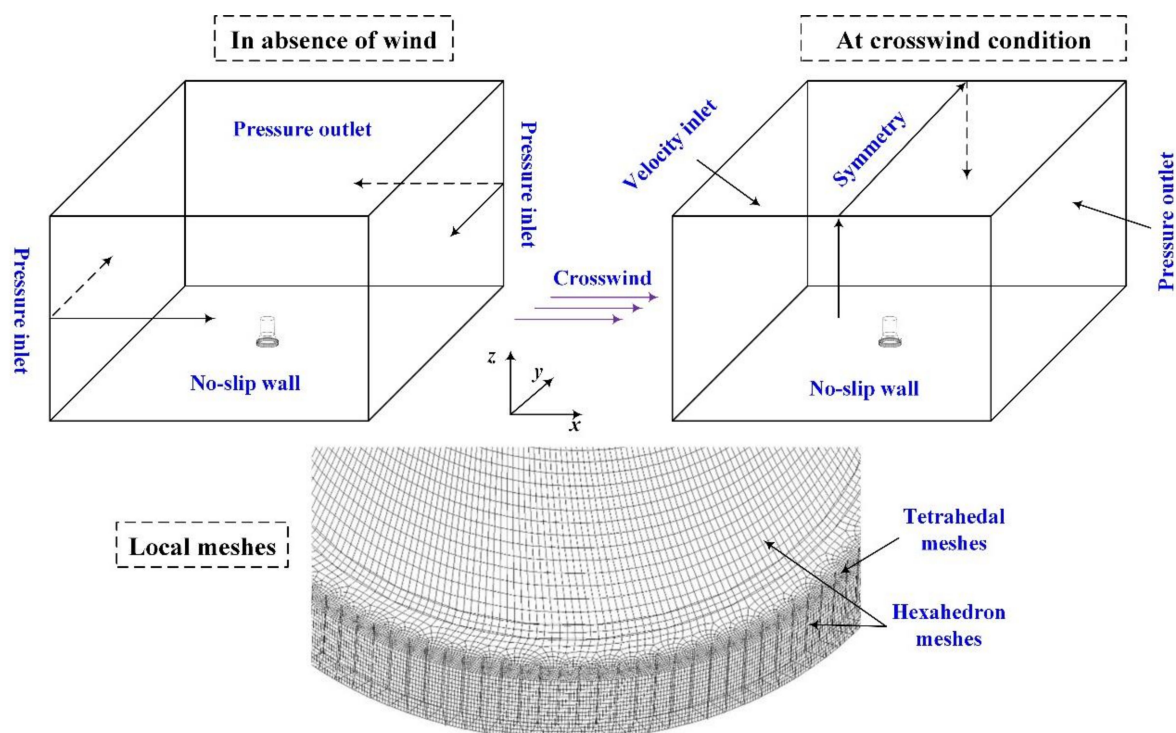


Figure 3. Illustrative computational domain of tower 2 with conical/cylindrical configuration.

Under ambient crosswind, the velocity inlet condition was assigned for windward plane. Furthermore, the crosswind speed as u_{wind} at height from the ground z m was computed by Equation (10) with the power-law function [9]:

$$u_{\text{wind}} = u_{\text{ref}} \left(\frac{z}{10} \right)^e \quad (10)$$

where u_{ref} means the referential crosswind at 10 m, which has five typical values: 4 m/s, 8 m/s, 12 m/s, 16 m/s, and 20 m/s. The factor e is given as 0.2 with regard to the roughness of the ground as well as the stability of the atmospheric condition. The downward plane is given as the pressure outlet condition; meanwhile, another two side planes and the top plane are all appointed as the symmetry condition. Without the ambient crosswind, the four side and top planes are given the pressure inlet and outlet boundary conditions, respectively. With respect to the ground, support pillars, as well as the tower shell, are given as the no slip wall condition. In addition, ambient temperature in this work was equal to 16 °C for the numerical modeling. During the numerical procedure, the divergence criterion

of the scaled residuals was 10^{-4} for the energy equation and 10^{-6} for the continuity and momentum equations [9,10].

During the numerical modeling, the heat transfer of the ambient air and water was coupled with the heat transfer of the water and exhausted steam. The water temperature drop in the steel-truss NDDCS equaled the water temperature rise in the condenser. In consequence, the numerical modeling was an iteration process. Furthermore, the determining parameter of convergence was taken as the coupled heat load of cooling system and condenser. The specific iterative steps for obtaining the thermal and flow performances of the steel-truss NDDCSs are displayed in Figure 4. At the design working condition of the coupled cold end system, the crosswind was 4 m/s, the turbine back pressure was 12 kPa, the heat flow rate was 224.5 MW, and the water flow rate was 6133.7 kg/s. First, the heat rejection of the condenser was acquired according to the heat transfer balance principle of the exhausted steam and circulating water. We input the obtained mean circulating water temperature in the numerical model of the cooling system and then obtained its heat rejection following the heat transfer balance principle of the circulating water and ambient air. Finally, we compared the heat rejections of the condenser and cooling system; if the relative error was not satisfied, we restarted the procedure again.

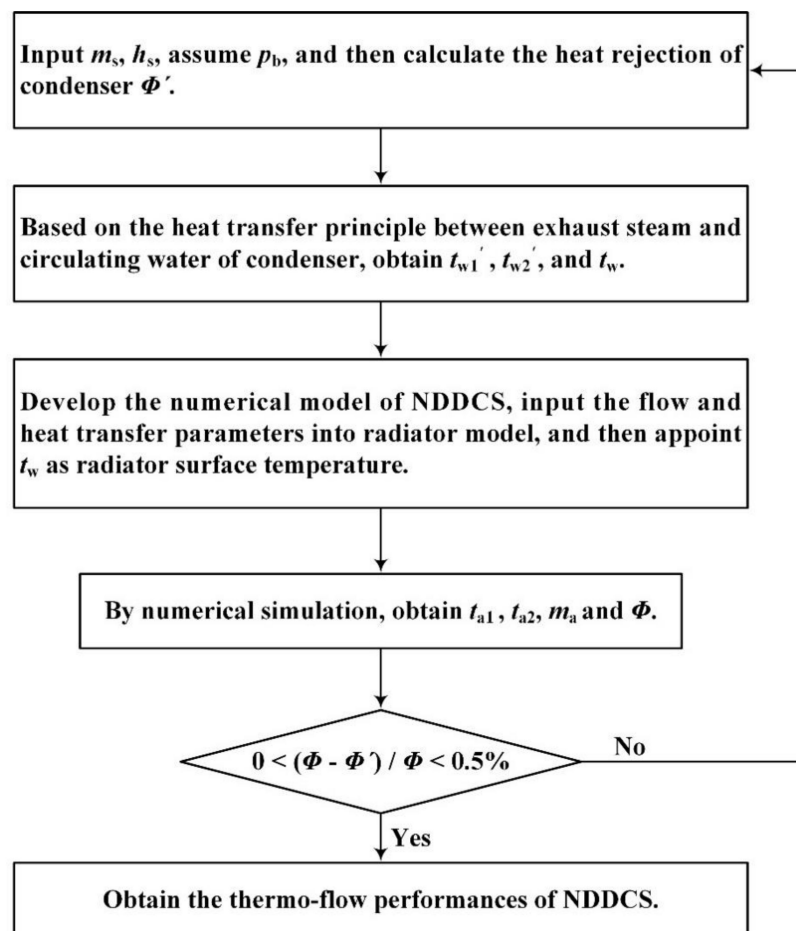


Figure 4. Numerical iteration process for various steel-truss cooling systems.

2.4. Experimental Validation

In our previous works, the wind tunnel experiment for NDDCS with the perpendicularly deployed ACHE underneath the cooling tower was carried out based on the similarity principle [2,14,17]. Figure 5 presents the distribution of the measuring positions in the cooling tower; meanwhile, the air flow velocities at the condition without wind and under crosswind of 4 m/s are provided.

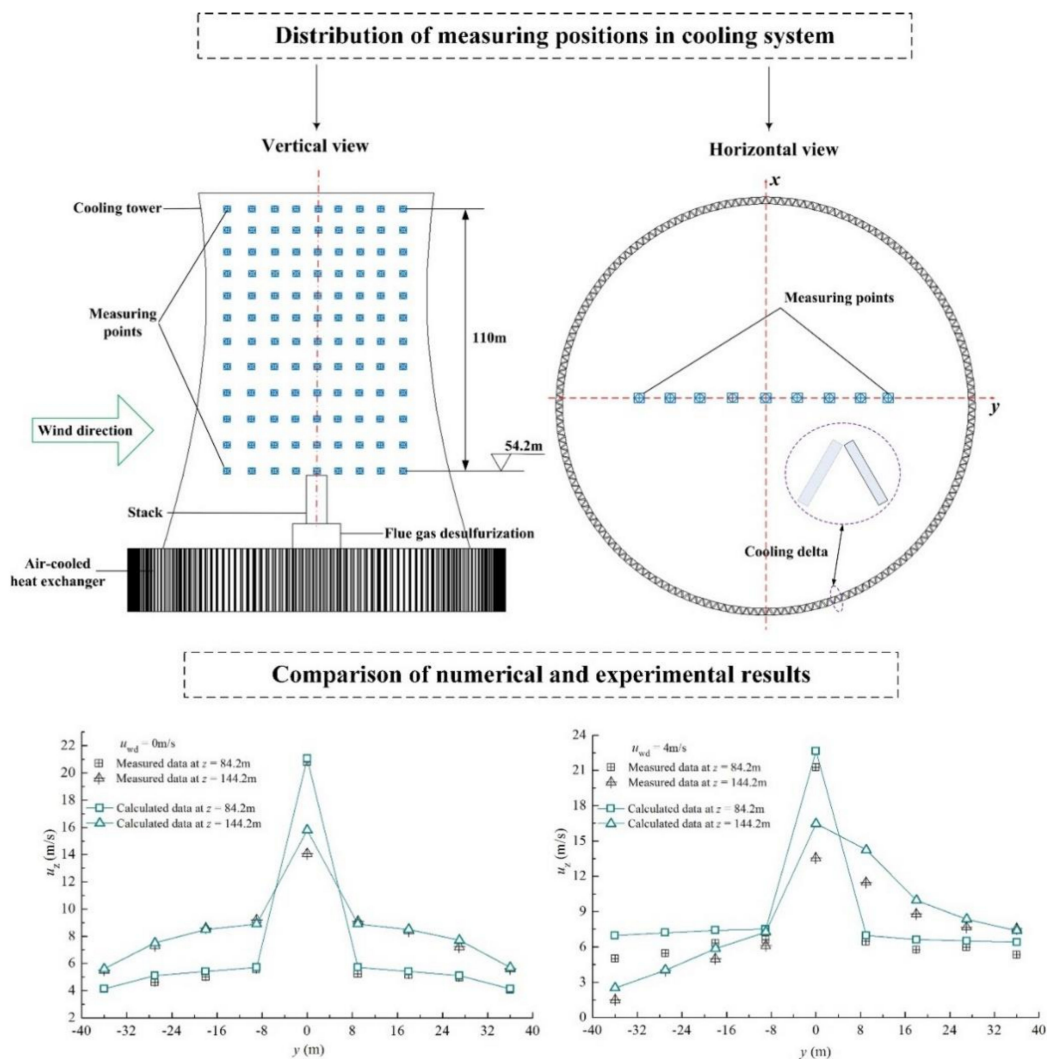


Figure 5. Distribution of the measuring positions in cooling tower and the comparison of the numerical and experimental air flow velocities [2,14,17].

The vertical heights of 84.2 m and 144.2 m were selected to be the illustrative cases for comparing the numerical and experimental results. As distinctly observed, both numerical and experimental air flow velocities in the center position were shown to be obviously larger than other positions because of the driving effects of flue gas plume. Without ambient wind, the air flow velocity in center position at 144.2 m was lower than that at 84.2 m. Under the crosswind of 4 m/s, the largest air flow velocity, at a height of 144.2 m, deviated to the downstream due to the blocking impact of the ambient wind. The numerical results always presented the same trend with the experimental data, and they agreed well with each other at both typical ambient conditions. The compared results imply that the numerical modeling and method can solve the thermal and flow process of NDDCS accurately, which provides validation support for this research with the same numerical procedure.

3. Results and Discussion

3.1. Thermal and Flow Fields

The pressure, flow, and also temperature contours were presented to reveal the thermal and flow characteristics of the steel-truss NDDCSs with the four typical engineering tower configurations. As in specific illustrations, the variable contours without ambient wind and under the design crosswind of 4 m/s are provided and explained in depth.

3.1.1. Without Ambient Wind

Figures 6–9 display the air variable contours of steel-tower NDDCSs with the four typical tower configurations in the absence of wind. For all tower configuration cases, the uniform reverse pressure gradients inside the cooling tower are formed to overcome the air flow resistance of ACHE, and then the centrally symmetric air flow and temperature fields are generated. With regard to tower 1, shown in Figure 6, the pressure difference between the inner and outer sides of ACHE was nearly 45 Pa. The reverse pressure near the ACHE and the bottom of cooling tower ranged from -15 Pa to -3 Pa. As for tower 2, Figure 7 presents the pressure difference, which equaled about 33 Pa, and was slightly lower than tower 1. In addition, the reverse pressure area was also smaller. Additionally, the air temperature contours of tower 1 and tower 2 were almost the same. Tower 3 in Figure 8 had similar temperature and pressure contours to tower 1. The slightly decreased flow and temperature fields of tower 2 and tower 3 came from the declined air flow stability with the only cylindrical section near the tower outlet, while tower 4, with the cylindrical configuration, showed an obviously smaller pressure difference in the ACHE, only 28 Pa. Furthermore, the big vortices also emerged adjacent to the turning corner near the tower bottom, and the phenomena ultimately incurred hot air recirculation, as observed in Figure 9. The seriously deteriorated air variable fields were caused by the sudden change of air flow direction with the sharp corner.

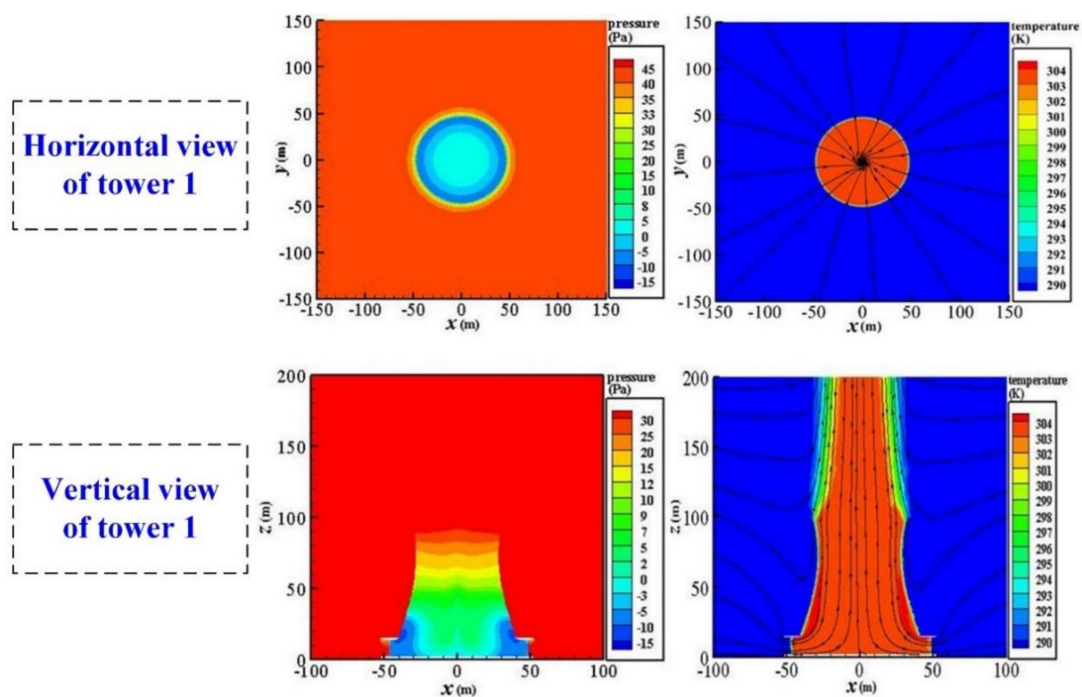


Figure 6. Air variable contours for steel-truss NDDCS with hyperbolic tower configuration without ambient wind.

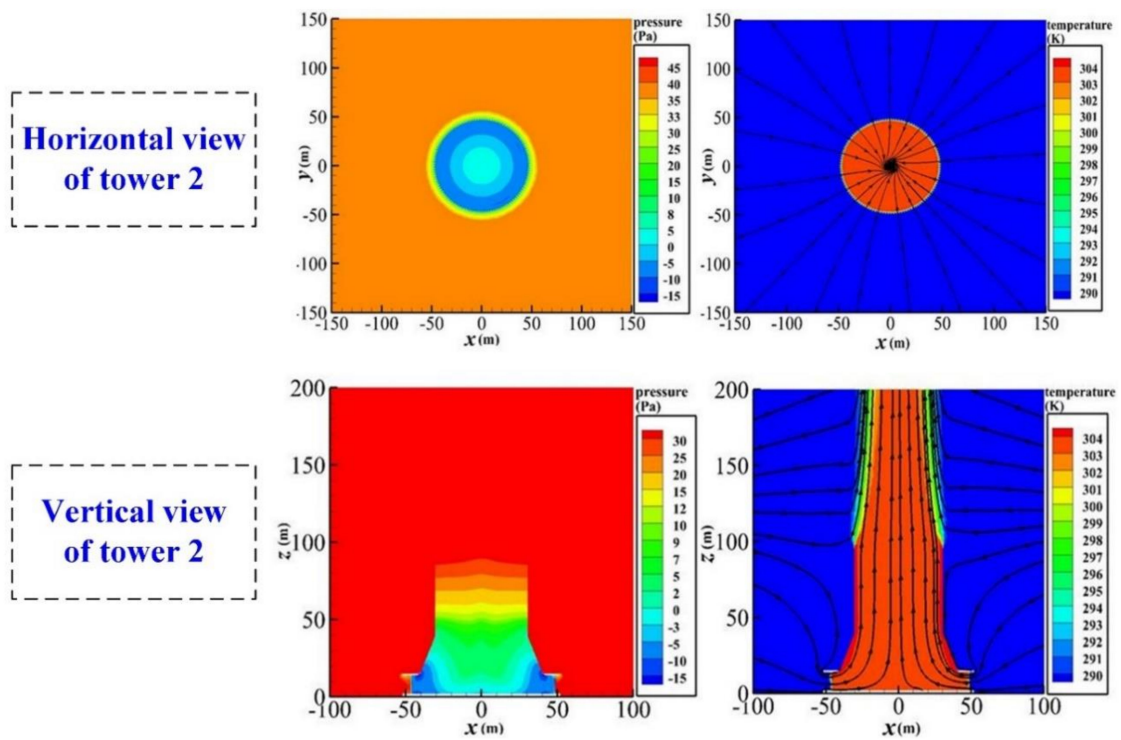


Figure 7. Air variable contours for steel-truss NDDCS with conical/cylindrical tower configuration without ambient wind.

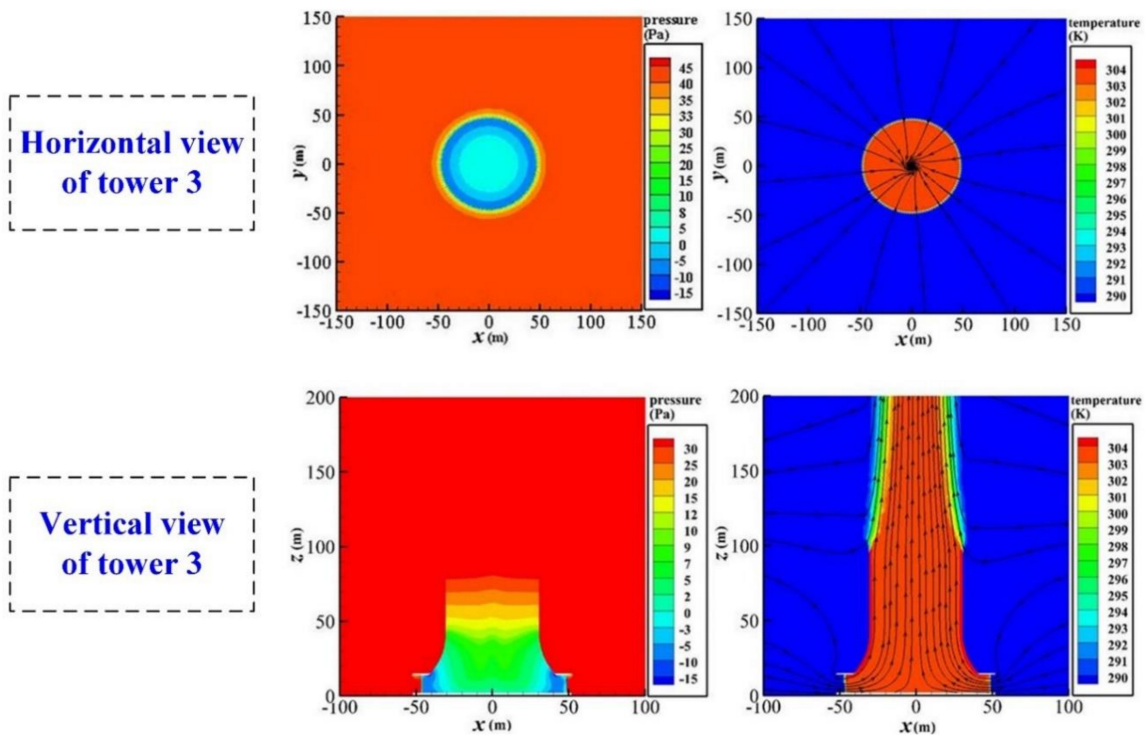


Figure 8. Air variable contours for steel-truss NDDCS with hyperbolic/cylindrical tower configuration without ambient wind.

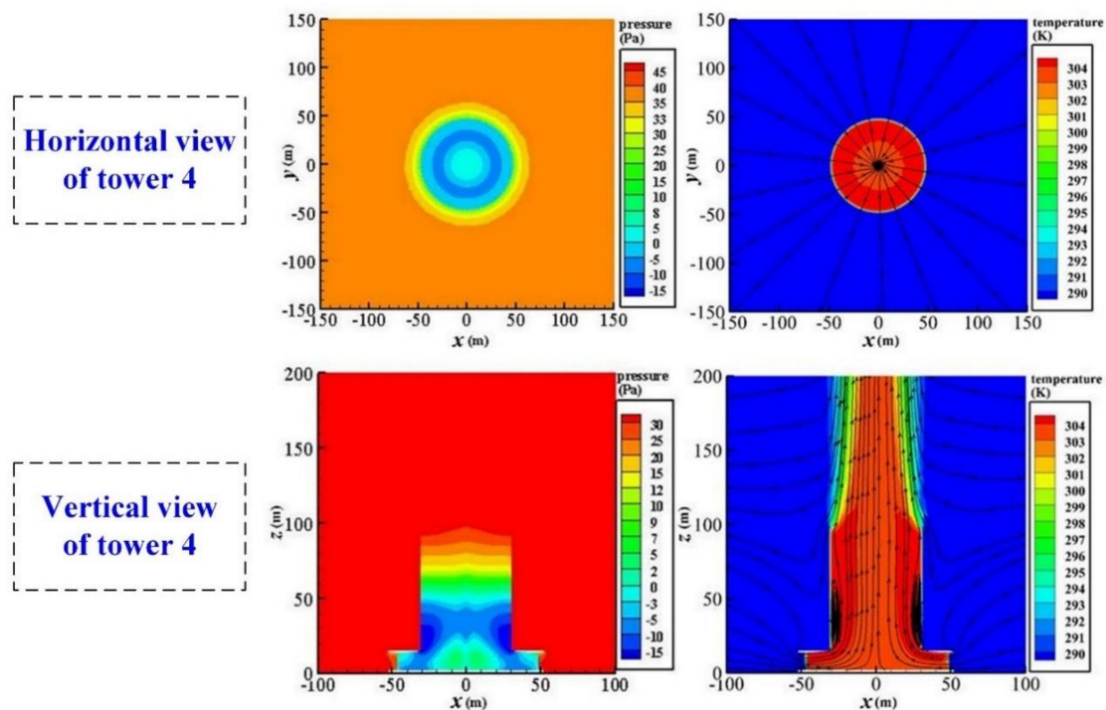


Figure 9. Air variable contours for steel-truss NDDCS with cylindrical tower configuration without ambient wind.

3.1.2. At Design Crosswind of 4 m/s

Figures 10–13 show the air variable contours for steel-tower NDDCSs with the four typical tower configurations under a design ambient wind of 4 m/s. With various tower configurations, cooling systems always present larger pressure differences in the windward air-cooled sectors compared to the lateral and leeward ones. Furthermore, the air flow discharge at the tower exit became weak due to the crosswind impacts. Compared to tower 1, tower 2 had a relatively smaller high-pressure area near the windward air-cooled sectors, while the low-pressure area near the lateral air-cooled sectors became slightly larger, as shown in Figures 10 and 11. Consequently, for tower 2 configuration, the air outlet temperature of the windward sectors appeared lower, whereas it was shown to be higher in the lateral air-cooled sectors. Additionally, some reverse flows emerged near the tower outlet because of the decreased pressure increase effects, which lead to adverse effects on the air mass flow rate. These variable phenomena imply that the conical/cylindrical configuration may have a lower cooling efficiency when compared with the traditional tower configuration. It can be seen in Figure 12, tower 3 had nearly similar air variable contours with tower 1, while the vertical view exhibited the reverse flow with vortex near the tower outlet. Tower 4, as given in Figure 13, presented an evidently lower pressure difference and air outlet temperature near the windward sectors. Meanwhile, the outlet air temperature near the lateral and leeward air-cooled sectors became apparently higher. Furthermore, the big vortices were generated near the tower outlet, which will cripple air flow significantly. Such adverse thermo-flow fields originated from significantly decreased buffering effects. These air flow and temperature fields predicted that the completely cylindrical tower configuration would have negative impact on the thermal process of the steel-truss NDDCS. Concluding from those aforementioned analyses, the traditional hyperbolic cooling tower/s possesses better cooling performance than the other tower configurations.

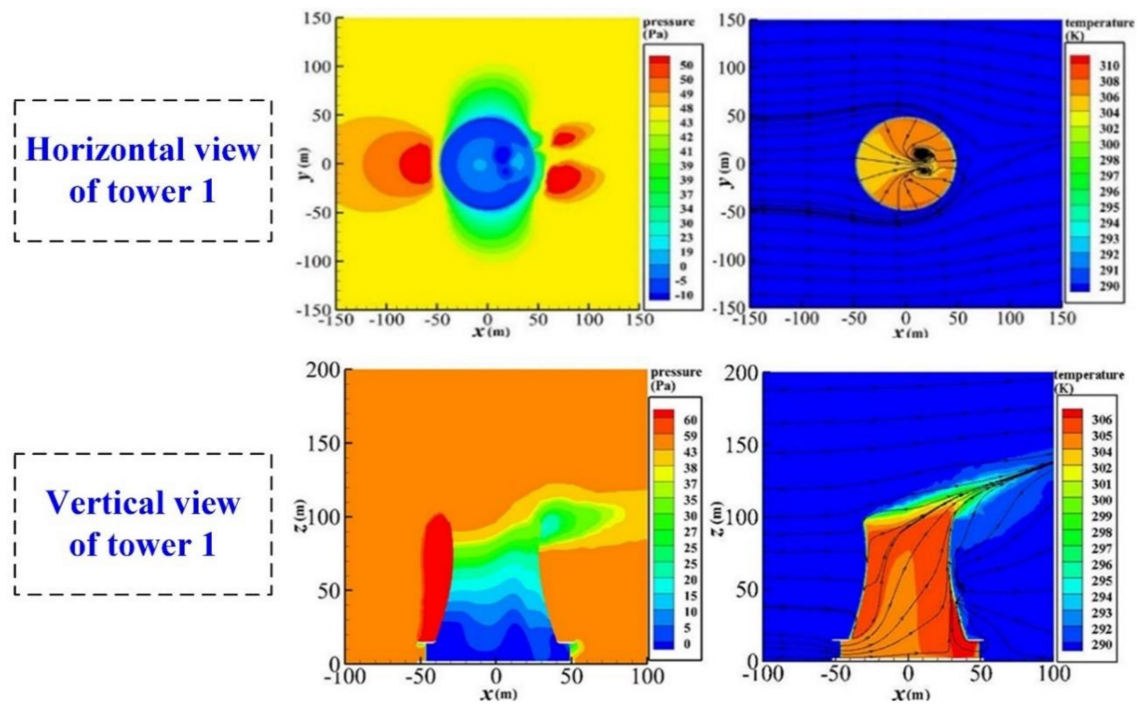


Figure 10. Air variable contours for steel-truss NDDCS with hyperbolic tower configuration at design crosswind of 4 m/s.

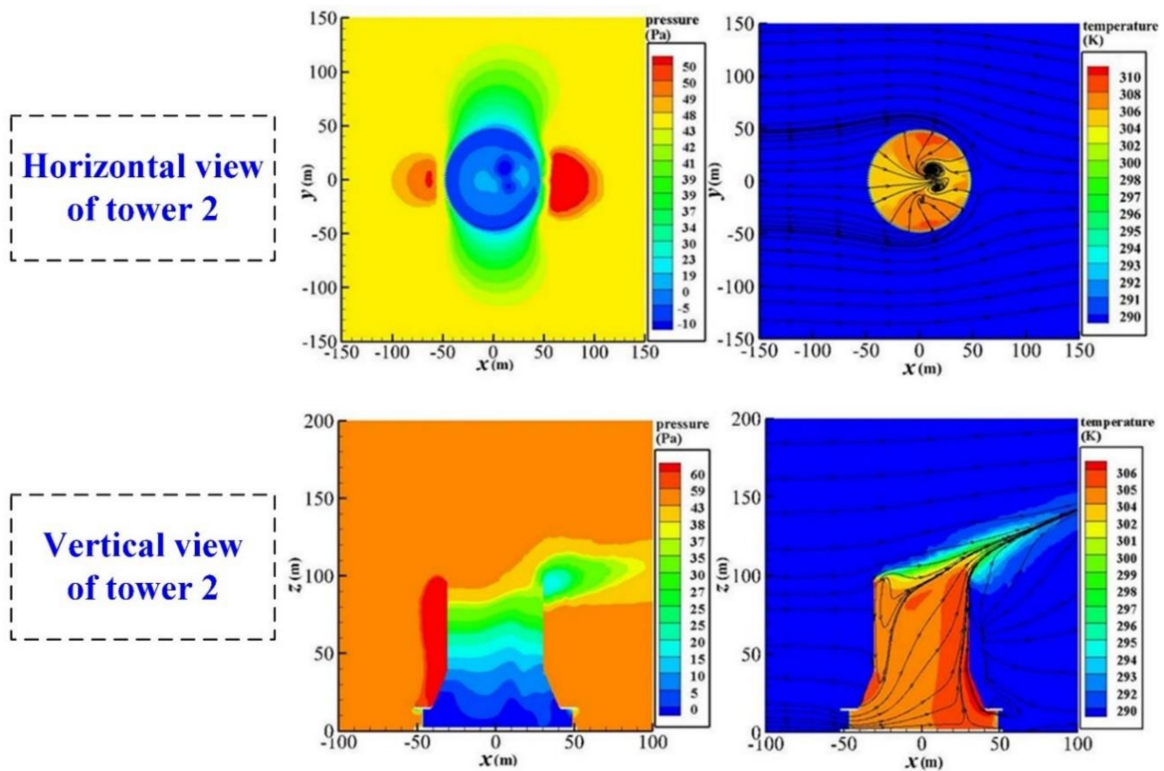


Figure 11. Air variable contours for steel-truss NDDCS with conical/cylindrical tower configuration at design crosswind of 4 m/s.

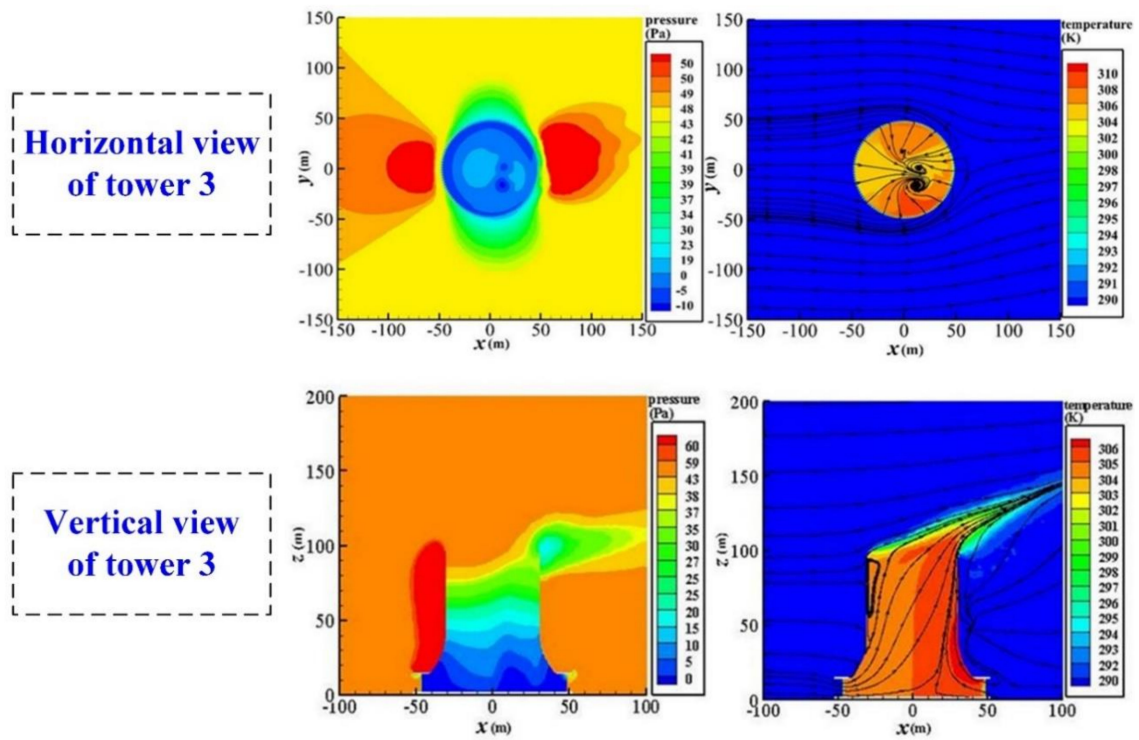


Figure 12. Air variable contours for steel-truss NDDCS with hyperbolic/cylindrical tower configuration at design crosswind of 4 m/s.

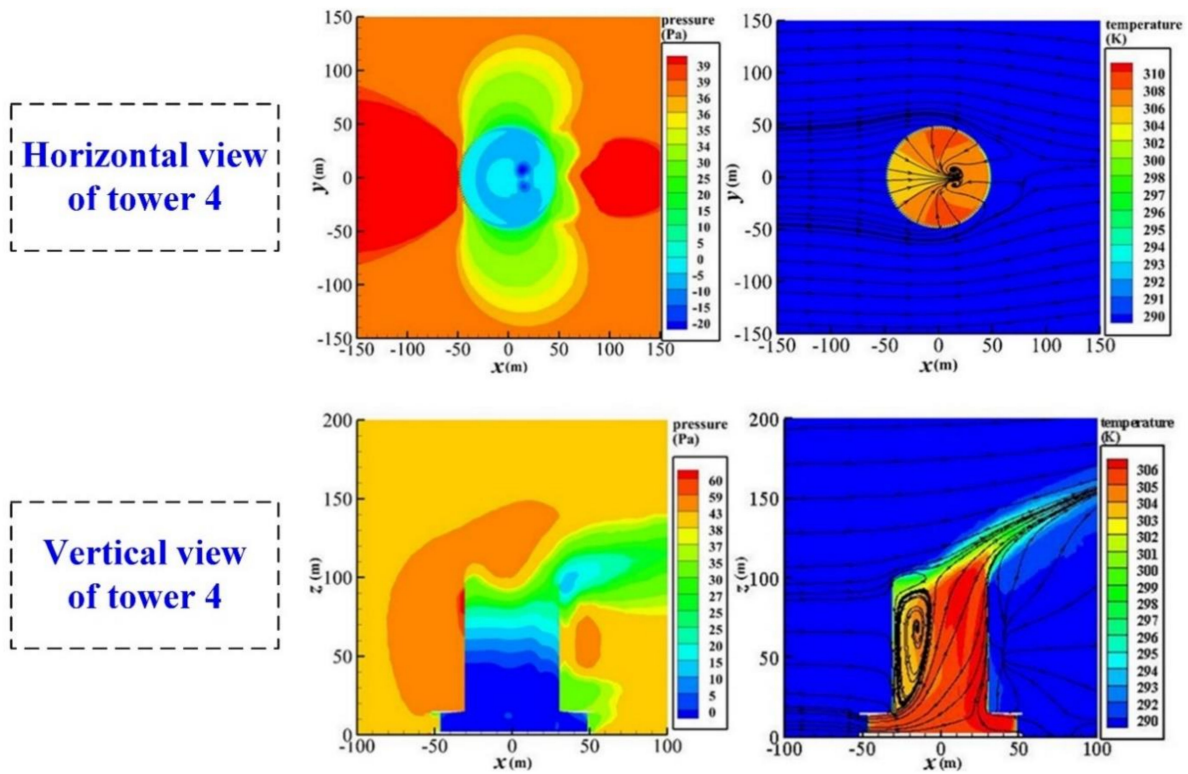


Figure 13. Air variable contours for steel-truss NDDCS with cylindrical tower configuration at design crosswind of 4 m/s.

3.2. Distributions of Local Thermal and Flow Behaviors

Based on those aforementioned variable contours, the mass flow of cooling air, as well as the heat rejection for the local sectors, are presented in Figure 14 for both the tower 1 configuration and the tower 4 configuration. These two steel-truss natural draft dry cooling systems had similar thermo-flow distributions among various air-cooled sectors. This implies that the tower configuration will not change the influencing trend of the crosswind on ACHE. As can also be observed, when the ambient wind became strengthened, the air flow and cooling capability for the windward sectors No. 5 and No. 6 increased, which, however, dropped heavily for the lateral sectors No. 3 and No. 8. In addition, compared with tower 1, tower 4, with the cylindrical configuration, had apparently declined thermal and flow results for nearly all local sectors, which verified the aforementioned air variable contours.

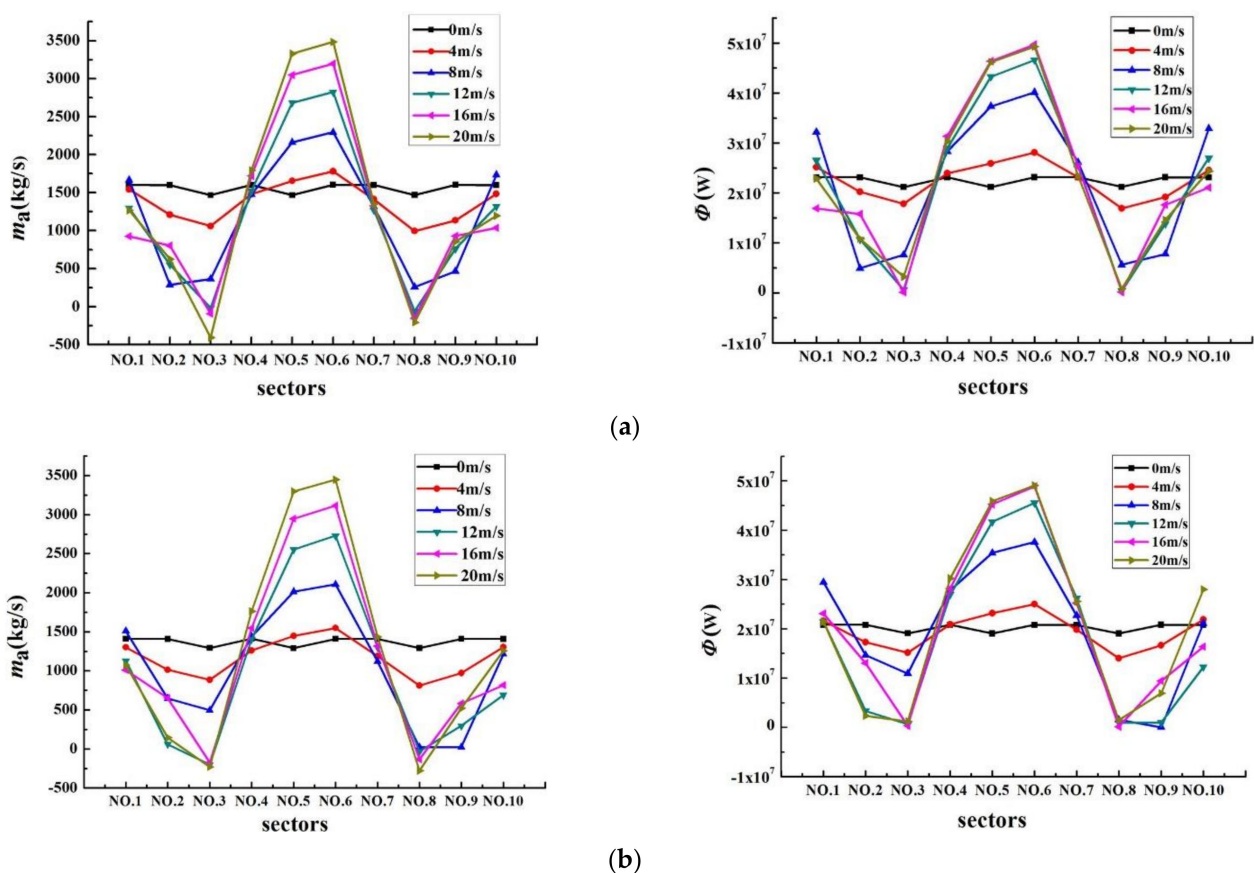


Figure 14. Distributions of local thermal and flow behaviors for air-cooled sectors of tower 1 configuration and tower 4 configuration. (a) Tower 1; (b) tower 4.

3.3. Comparisons of Overall Thermal and Flow Performances

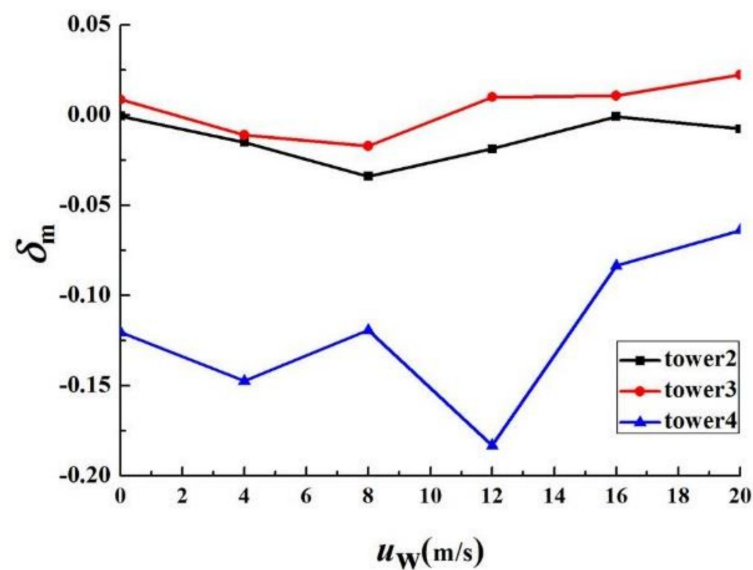
The dimensionless parameters of the total air flow rate δ_m and also the total heat transfer rate δ_ϕ are given for comparing the overall thermal and flow behaviors of the four steel-truss NDDCSs with the typical cooling tower configurations.

$$\delta_m = \frac{m_{ai} - m_{a1}}{m_{a1}} \times 100\% \quad (11)$$

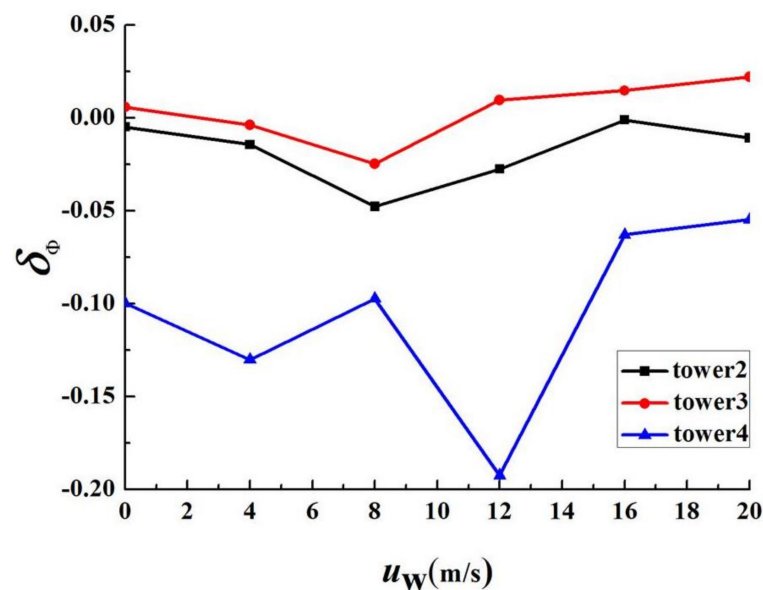
$$\delta_\phi = \frac{\Phi_i - \Phi_1}{\Phi_1} \times 100\% \quad (12)$$

where m_{a1} and Φ_1 represent the total air flow rate and also the total heat transfer rate for tower 1 with the traditional hyperbolic configuration, meanwhile m_{ai} and Φ_i mean the total air flow rate and the total heat rejection for other tower configurations.

The comparisons of the overall thermal and flow performances for the four steel-truss NDDCSs under various ambient wind conditions are provided. It can be concluded from Figure 15 that both non-dimensional air flow rate and heat transfer rate for tower 2 were a little negative, resulting from the slightly worse air variable fields. Tower 3 had the better cooling performance under the high crosswinds, which differed from the results under other crosswind conditions; whereas, for tower 4, the thermo-flow performance was shown to be apparently worse than the other tower configurations with much lower negative parameters.



(a)



(b)

Figure 15. Comparisons of the overall thermal and flow parameters for the four tower configurations. (a) Non-dimensional total mass flow of cooling air; (b) non-dimensional total heat transfer rate.

4. Conclusions

This investigation paid attention to the thermal and flow behaviors for the steel-truss NDDCSs with four typical engineering tower configurations by numerical modeling. For these steel-truss natural draft dry cooling systems, the air variable contours were analyzed, the local air flow rate and heat transfer rate were presented, and the overall thermal and flow performances were compared. The main findings are summarized as follows:

- (1) In absence of wind, tower 2 presented slightly lower pressure difference in ACHE than tower 1. Tower 3 had similar pressure and temperature fields with tower 1, while tower 4 showed a much smaller pressure difference, and the big vortices also emerged adjacent to the turning corner of cooling tower.
- (2) At a design crosswind of 4 m/s, tower 2 displayed a smaller area of high pressure near the windward sectors, It also had a larger area of low pressure near the lateral sectors than tower 1. The vertical air flow fields of tower 3 showed some reverse flows with vortices near the tower outlet, which became fairly big inside tower 4.
- (3) Tower configuration did not change the trend of crosswind impacts on ACHE. Compared with tower 1, tower 4 had apparently lower air flow rate and heat transfer rate for nearly all local sectors.
- (4) The non-dimensional thermal and flow parameters of tower 2 were slightly negative, whereas, tower 3 presented better cooling performance under high crosswinds. Tower 4 had the worst overall thermo-flow performances compared with the other tower configurations.

For engineering application of the steel-truss natural draft dry cooling system, the traditional hyperbolic tower configuration is recommended for areas with a commonly small crosswind, while for those regions with frequently high crosswinds, the hyperbolic/cylindrical tower configuration is preferred.

Author Contributions: Conceptualization, H.G. and W.W.; methodology, T.C.; software, Y.Y. and H.Z.; formal analysis, H.G.; resources, W.W.; writing—original draft preparation, W.W.; writing—review and editing, W.W.; supervision, X.D.; project administration, X.D. All authors have read and agreed to the published version of the manuscript.

Funding: This research received no external funding.

Acknowledgments: The financial supports for this research, from the National Natural Science Foundation of China (Grant No. 52006055) and the Basic Research Foundation of Central Universities (Grant No. 2019QN023), are gratefully acknowledged.

Conflicts of Interest: The authors declare no conflict of interest.

Nomenclature

<i>D</i>	diameter (m)
<i>H</i>	height (m)
<i>H</i>	convective heat transfer coefficient ($W m^{-2} K^{-1}$)
<i>K</i>	flow loss coefficient
<i>L</i>	tube length (m)
<i>M</i>	molecular weight ($g mol^{-1}$)
<i>M</i>	mass flow rate ($kg s^{-1}$)
<i>N</i>	Number
<i>P</i>	pressure (Pa)
<i>R</i>	universal gas constant ($J mol^{-1} K^{-1}$)
<i>S</i>	source term in generic equation
<i>t</i>	temperature (K)
<i>u</i>	velocity ($m s^{-1}$)
<i>V</i>	volume (m^3)
<i>x</i>	coordinate axis

Greek symbols

Γ	diffusion coefficient ($\text{m}^2 \text{s}^{-1}$)
Φ	heat rejection rate (W)
φ	scalar variable
ρ	density (kg m^{-3})

Subscripts

a	Air
j	coordinate direction
ref	Reference
wind	Crosswind
wa	Water
1	Inlet
2	Outlet

Acronyms

ACHE	air-cooled heat exchanger
NDDCS	natural draft dry cooling system

References

- Li, X.X.; Gurgenci, H.; Guan, Z.Q.; Wang, X.R.; Xia, L. A review of the crosswind effect on the natural draft cooling towers. *Appl. Therm. Eng.* **2019**, *150*, 250–270. [[CrossRef](#)]
- Wang, W.J.; Yang, L.J.; Du, X.Z.; Yang, Y.P. Anti-freezing water flow rates of various sectors for natural draft dry cooling system under wind conditions. *Int. J. Heat Mass Transf.* **2016**, *102*, 186–200. [[CrossRef](#)]
- Yu, Q.Q.; Gu, X.L.; Li, Y.; Lin, F. Collapse-resistant performance of super-large cooling towers subjected to seismic actions. *Eng. Struct.* **2016**, *102*, 77–89. [[CrossRef](#)]
- Ma, H.H.; Li, Z.Y.; Li, S.Z.; San, B.B.; Fan, F. Stability analysis and performance comparison of large-scale hyperbolic steel cooling towers with different latticed shell systems. *J. Constr. Steel Res.* **2019**, *160*, 559–578. [[CrossRef](#)]
- Ma, H.H.; Zhao, Y.; Fan, F.; Yu, Z.W.; Zhi, X.D. Experimental and numerical study of new connection systems for a large-span hyperbolic steel cooling tower. *Eng. Struct.* **2019**, *195*, 452–468. [[CrossRef](#)]
- Ma, T.T.; Zhao, L.; Chen, N.Y.; Ge, Y.J.; Zhang, D. Wind-induced dynamic performance of a super-large hyperbolic steel-truss cooling tower. *Thin-Walled Struct.* **2020**, *157*, 107061. [[CrossRef](#)]
- Ma, H.H.; Li, S.Z.; Fan, F. Static performance analysis of single-layer steel cooling tower. *Structures* **2019**, *19*, 322–332. [[CrossRef](#)]
- Song, G.Q.; Zhi, X.D.; Fan, F.; Wang, W.; Wang, P. Cooling performance of cylinder-frustum natural draft dry cooling tower. *Appl. Therm. Eng.* **2020**, *180*, 115797. [[CrossRef](#)]
- Zhao, Y.B.; Long, G.Q.; Sun, F.Z.; Li, Y.; Zhang, C.J. Numerical study on the cooling performance of dry cooling tower with vertical two-pass column radiators under crosswind. *Appl. Therm. Eng.* **2015**, *75*, 1106–1117. [[CrossRef](#)]
- Zhao, Y.B.; Sun, F.Z.; Li, Y.; Long, G.Q.; Yang, Z. Numerical study on the cooling performance of natural draft dry cooling tower with vertical delta radiators under constant heat load. *Appl. Energy* **2015**, *149*, 225–237. [[CrossRef](#)]
- Ma, H.; Si, F.Q.; Kong, Y.; Zhu, K.P.; Yan, W.S. A new theoretical method for predicating the part-load performance of natural draft dry cooling towers. *Appl. Therm. Eng.* **2015**, *78*, 1106–1115. [[CrossRef](#)]
- Li, X.X.; Gurgenci, H.; Guan, Z.Q.; Sun, Y.B. Experimental study of cold inflow effect on a small natural draft dry cooling tower. *Appl. Therm. Eng.* **2018**, *128*, 762–771. [[CrossRef](#)]
- Goodarzi, M.; Amooie, H. Heat transfer enhancement in a natural draft dry cooling tower under crosswind operation with heterogeneous water distribution. *Int. J. Nucl. Power* **2016**, *61*, 252–259.
- Wang, X.B.; Yang, L.J.; Du, X.Z.; Yang, Y.P. Performance improvement of natural draft dry cooling system by water flow distribution under crosswinds. *Int. J. Heat Mass Transf.* **2017**, *108*, 1924–1940. [[CrossRef](#)]
- Li, X.X.; Xia, L.; Gurgenci, H.; Guan, Z.Q. Performance enhancement for the natural draft dry cooling tower under crosswind condition by optimizing the water distribution. *Int. J. Heat Mass Transf.* **2017**, *107*, 271–280. [[CrossRef](#)]
- Zhao, Y.B.; Long, G.Q.; Sun, F.Z.; Li, Y.; Zhang, C.J.; Liu, J.B. Effect mechanism of air deflectors on the cooling performance of dry cooling tower with vertical delta radiators under crosswind. *Energy Convers. Manag.* **2015**, *93*, 321–331. [[CrossRef](#)]
- Chen, L.; Yang, L.J.; Du, X.Z.; Yang, Y.P. Performance improvement of natural draft dry cooling system by interior and exterior windbreaker configurations. *Int. J. Heat Mass Transf.* **2016**, *96*, 42–63. [[CrossRef](#)]
- Gu, H.F.; Wang, H.J.; Gu, Y.Q.; Yao, J.N. A numerical study on the mechanism and optimization of wind-break structures for indirect air-cooling towers. *Energy Convers. Manag.* **2016**, *108*, 43–49. [[CrossRef](#)]
- Wang, W.L.; Zhang, H.; Li, Z.; Lv, J.F.; Ni, W.D.; Li, Y.S. Adoption of enclosure and windbreaks to prevent the degradation of the cooling performance for a natural draft dry cooling tower under crosswind conditions. *Energy* **2016**, *116*, 1360–1369. [[CrossRef](#)]
- Wang, W.L.; Zhang, H.; Liu, P.; Li, Z.; Lv, J.F.; Ni, W.D. The cooling performance of a natural draft dry cooling tower under crosswind and an enclosure approach to cooling efficiency enhancement. *Appl. Energy* **2017**, *186*, 336–346. [[CrossRef](#)]
- Ma, H.; Si, F.Q.; Kong, Y.; Zhu, K.P.; Yan, W.S. Wind-break walls with optimized setting angles for natural draft dry cooling tower with vertical radiators. *Appl. Therm. Eng.* **2017**, *112*, 326–329. [[CrossRef](#)]

22. Ma, H.; Si, F.Q.; Zhu, K.P.; Wang, J.S. The adoption of windbreak wall partially rotating to improve thermo-flow performance of natural draft dry cooling tower under crosswind. *Int. J. Therm. Sci.* **2018**, *134*, 66–88. [[CrossRef](#)]
23. Wu, T.; Ge, Z.H.; Yang, L.J.; Du, X.Z. Flow deflectors to release the negative defect of natural wind on large scale dry cooling tower. *Int. J. Heat Mass Transf.* **2019**, *128*, 248–269. [[CrossRef](#)]
24. Xia, L.; Gurgenci, H.; Liu, D.Y.; Guan, Z.Q.; Zhou, L.; Wang, P. CFD analysis of pre-cooling water spray system in natural draft dry cooling towers. *Appl. Therm. Eng.* **2016**, *105*, 1051–1060. [[CrossRef](#)]
25. Chen, L.; Huang, X.W.; Yang, L.J.; Du, X.Z.; Yang, Y.P. Evaluation of natural draft dry cooling system incorporating water spray air precooling. *Appl. Therm. Eng.* **2019**, *151*, 294–307. [[CrossRef](#)]
26. Huang, X.W.; Chen, L.; Yang, L.J.; Du, X.Z.; Yang, Y.P. Evaporation aided improvement for cooling performance of large scale natural draft dry cooling system. *Appl. Therm. Eng.* **2019**, *163*, 114350. [[CrossRef](#)]
27. Dong, P.X.; Li, X.X.; Sun, Y.B.; Hooman, K.; Guan, Z.Q.; Dai, Y.C.; Gurgenci, H. Numerical investigation of the influence of local effects on the transient start-up process of natural draft dry cooling towers in dispatchable power plants. *Int. J. Heat Mass Transf.* **2019**, *133*, 166–178. [[CrossRef](#)]
28. Dong, P.X.; Li, X.X.; Hooman, K.; Sun, Y.B.; Li, J.S.; Guan, Z.Q.; Gurgenci, H. The crosswind effects on the start-up process of natural draft dry cooling towers in dispatchable power plants. *Int. J. Heat Mass Transf.* **2019**, *135*, 950–961. [[CrossRef](#)]
29. Dai, Y.C.; Kaiser, A.S.; Lu, Y.S.; Klimenko, A.Y.; Dong, P.X.; Hooman, K. Addressing the adverse cold air inflow effects for a short natural draft dry cooling tower through swirl generation. *Int. J. Heat Mass Transf.* **2019**, *145*, 118738. [[CrossRef](#)]
30. Kong, Y.Q.; Wang, W.J.; Yang, L.J.; Du, X.Z.; Yang, Y.P. Water redistribution among various sectors to avoid freezing of air-cooled heat exchanger. *Int. J. Heat Mass Transf.* **2019**, *141*, 294–309. [[CrossRef](#)]
31. Wang, W.J.; Kong, Y.Q.; Huang, X.W.; Yang, L.J.; Du, X.Z.; Yang, Y.P. Anti-freezing of air-cooled heat exchanger by switching off sectors. *Appl. Therm. Eng.* **2017**, *120*, 327–339. [[CrossRef](#)]
32. Wang, W.J.; Huang, X.W.; Yang, L.J.; Du, X.Z.; Yang, Y.P. Anti-freezing operation strategies of natural draft dry cooling system. *Int. J. Heat Mass Transf.* **2018**, *118*, 165–170. [[CrossRef](#)]
33. Li, W.D.; Wang, H.T.; Wang, J.; Duan, C.P.; Zhao, Y.B. Effect mechanism of exit-water temperature distribution characteristics on the anti-freezing of natural draft dry cooling tower. *Appl. Therm. Eng.* **2019**, *161*, 114078. [[CrossRef](#)]
34. Ma, H.; Si, F.Q.; Zhu, K.P.; Wang, J.S. Utilization of partial through-flow tower shell to cope with the excess cooling capacity of dry cooling tower in extremely cold days with crosswind. *Int. J. Therm. Sci.* **2019**, *136*, 70–85. [[CrossRef](#)]
35. Zhou, J.X.; Ma, H.; Si, F.Q.; Zhu, K.P.; Wang, J.S. To broaden safe operation range of the indirect dry cooling system with internal annular windbreak cloth in extremely cold days. *Appl. Therm. Eng.* **2019**, *152*, 420–429. [[CrossRef](#)]
36. Hong, G.; Kim, C.; Hong, J. Energy conservation potential of economizer controls using optimal outdoor air fraction based on field study. *Energies* **2020**, *13*, 5038. [[CrossRef](#)]
37. Shumaev, V.V.; Kuzenov, V.V. Development of the numerical model for evaluating the temperature field and thermal stresses in structural elements of aircrafts. *J. Phys. Conf. Ser.* **2017**, *891*, 012311. [[CrossRef](#)]
38. Ryzhkov, S.V.; Kuzenov, V.V. Analysis of the ideal gas flow over body of basic geometrical shape. *Int. J. Heat Mass Transf.* **2019**, *132*, 587–592. [[CrossRef](#)]